INTERNATIONAL JOURNAL OF
ENERGY AND ENVIRONMENT

Volume 5, Issue 2, 2014 pp.155-182
Journal homepage: www.IJEE.IEEFoundation.org

Experimental study on a simplified crossflow turbine

Chiyembekezo S. Kaunda[1], Cuthbert Z. Kimambo[2], Torbjorn K. Nielsen[1]

[1] Waterpower Laboratory, Department of Energy and Process Engineering, Norwegian University of Science and Technology, Trondheim 7491, Norway.
[2] Department of Mechanical and Industrial Engineering, University of Dar es Salaam, P.O. Box 35091, Dar es Salaam, Tanzania.

Abstract
The main aim of the study is to enhance the design of a Crossflow turbine, as an appropriate technology for small-scale power generation. This study evaluates the performance of a simplified Crossflow turbine at conditions other than the 'best efficiency point'. It also explores the 'reaction' behavior of the Crossflow turbine as well as characterizes the torque transfer in the two stages of the turbine.
The experiments were conducted on a physical simplified Crossflow turbine model using the test facilities in the Waterpower Laboratory at the Norwegian University of Science and Technology. The results show that the maximum turbine efficiency is 79%, achieved at a head of 5m and reduced speed of 13.4; making it a low speed turbine. This turbine efficiency compares well with some reported efficiency values. The result also show that the turbine is efficient when it operates with a degree of reaction and this is achieved at large valve openings; validating observations that the Crossflow turbine is not a pure impulse turbine. Performance evaluation outside the best efficiency point shows that the efficiency decreases with increase in head above the best efficiency head. The turbine efficiency is not sensitive to flow variations: except at a head of 3m, at all tested heads, 25% of the flow at best efficiency point still generates efficiency of above 50%.
Torque characterization shows that the second stage plays a significant role in torque transfer, especially when at large valve openings. Therefore, design efforts must also look at how the flow inside the runner interior space can be controlled so that the jet enters the second stage with optimum flow angles. The use of strain gauge to characterize the torque produced using momentum principle as employed in this study presents an additional opportunity to analyze the trends in the torque transfer.

Keywords: Crossflow turbine; Small-scale hydropower; Appropriate technology; Crossflow turbine performance characterization; Crossflow turbine two two-stage torque characterization.

1. Introduction
Exploitation of renewable energy sources, such as micro hydropower for remote off-grid power supply is currently favored by many developing countries. A typical, micro hydropower system (less than 100 kW) is robust enough to supply electrical power for diverse application a remote location. The most critical component of a micro hydropower system is the turbine. The Crossflow turbine, also known as Banki turbine, is simple to design and manufacture. In an 'appropriate technology' manner, the runner blades can be cut from standard steel pipes. For this reason, Crossflow turbine technology has been promoted in developing countries, especially those in Asia, by charitable organizations such as Practical Action

(former Intermediate Technology), Swiss Centre for Appropriate Technology (SKAT) and German Organization for Technical Cooperation (GTZ).
Despite being simple to design, the crossflow turbines have relative low performances levels compared to other conventional turbines that are also used in microhydropower generation; such as Francis, Turgo and Pelton Wheel. The commercialization of Crossflow turbines has been hampered by most small-scale turbine manufactures' unwillingness to manufacture it, possibly on the reason of its underperformance. Therefore, the Crossflow turbine s one of the turbines that has not gone through a remarkable performance improvement as compared to the traditional mentioned turbines. The performance improvement activities are informed by a detailed performance evaluation studies.
Crossflow turbine is a two stage turbine and the contribution of power transfer in each stage has been a subject of theoretical and experimental investigation for some decades ago. The results significantly vary among investigators. Possibly the sources of variation may be the high levels of uncertainties associated with second stage power transfer, assumptions made during the theoretical analysis, different geometrical configurations of the Crossflow turbine testing models and the methodologies that were used.
The current experimental study focuses on a simplified version of a traditional Crossflow turbine where the flow control is no longer achieved by a special guidevane by a simple flap which is actuated manually by a screw operated handle. The turbine was designed using pure impulse principle.

1.1 Objectives
The objective of this paper is to performance experimental investigations on a simplified Crossflow turbine. Specifically, the study will:

- Develop performance characteristic curves for the Crossflow turbine and compare with other turbines used in micro hydropower projects.
- Explore the 'reaction' behavior of the turbine.
- Characterize the relative torque transfer and their patterns in the two stages.

The main aim of the study is to enhance the simplified design of the turbine which can be used as an appropriate technology for small scale power generation, especially in least developed countries.

2. Crossflow turbine

A hydraulic turbine converts hydraulic power into mechanical power in form of rotating shaft. The power transfer process takes place on the surfaces of the blades. The blades are assembled on a disc that is supported by a shaft; the whole assembly is technically known as runner. The runner the Crossflow turbine (CFT) runner consists of relatively longer circular blades in the transverse direction that are welded onto the two or more circular discs. The shaft of the CFT runner can be connected to the electric generator to produce electricity or it can be connected to any other work consuming device like a milling machine.
A typical CFT technology (such as in Figure1) consists of two main components namely the nozzle and the runner. The flow of water crosses the runner blades twice, from the periphery towards the centre, and after crossing the open centre space, from the inside to the outward periphery. This turbine is therefore a turbo-machine with two velocity stages, and water filling only part of the runner at any time of operation. The portion of water that crosses the runner twice is known as crossed-flow, and the name of the turbine is derived from this phenomenon. There is some portion of water is entrained within the runner blade and flung out of the runner tangentially. This is the entrained flow.
A nozzle, which converts potential energy to kinetic energy of the water in form of a high velocity jet, is an important component for impulse turbines. The CFT turbine nozzle is basically a rectangle in cross-section. The two surfaces are planes and the other two surfaces are typically curved. To guide and control water flow to the runner blades, the nozzle may incorporate a guidevane or the one of the nozzle curved surfaces can be made move movable to control the outlet Cross-sectional area.

2.1 Model Crossflow turbine description
The model turbine was designed and manufactured with the purpose of simplifying the traditional CFT with a guidevane and therefore reducing its cost further. The typical design equations for the sizing of the runner size and blade angles were employed. The important simplification to the traditional turbine is the use of adjustable valve that uses a plane flap controlled by the screw shaft to direct and control amount of the flow to the runner. This design eliminated the inclusion of a guidevane or the movable nozzle wall that require a special curve. The adjustable valve in this project has a disadvantage of requiring large

torque to operate the nozzle because of the large hydraulic force acting on the flap. But this can be overcome by employing a handle with a large radius. Further, the amount of water flows in micro hydropower applications are not relatively large for CFT and therefore the 'large amount' of torque required to operate the nozzle while the turbine is in operation would not call for the use of a servomotor. However, it is a concern during the turbine operation and should be addressed when designing the handle.

Figure 2 shows the schematic drawing of the simplified CFT. Figure 3 shows the pictorial view of the turbine. Table 1 shows the design parameters for the model simplified CFT turbine used in the experiment.

3. Theoretical framework

3.1 Efficiency determination and design parameter review

As this research deals with performance characterization of the simplified Crossflow turbine, it is important to describe the theory behind the turbine operation and determination of the performance parameters. Crossflow turbine was originally designed as an impulse turbine where there was a considerable gap between the nozzle outlet and runner. However, there have been some observations that with current modifications to the turbine where the nozzle follows the runner housing closely, presence of positive gauge pressure has been noted in runner first stage. This shows that energy transfer in the first stage might be due to reaction principle.

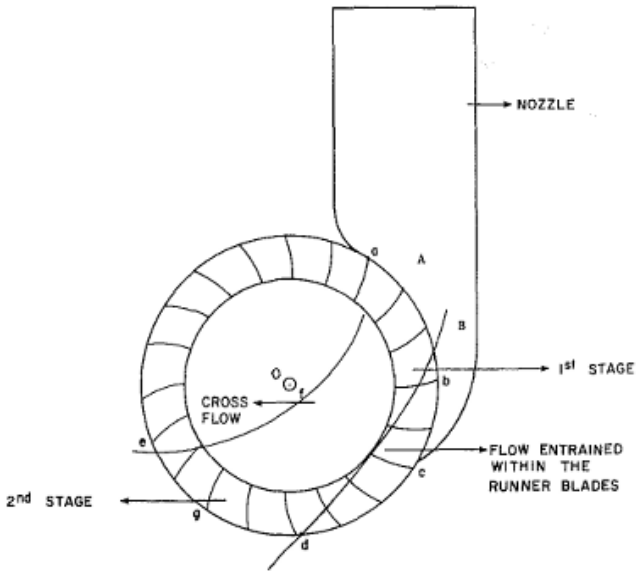

Figure 1. A schematic diagram of a typical Crossflow turbine showing nozzle, runner and flow pattern [1]

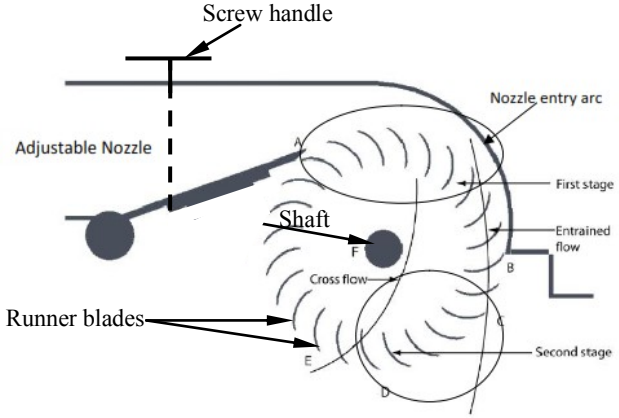

Figure 2. Schematic sketch of the model turbine

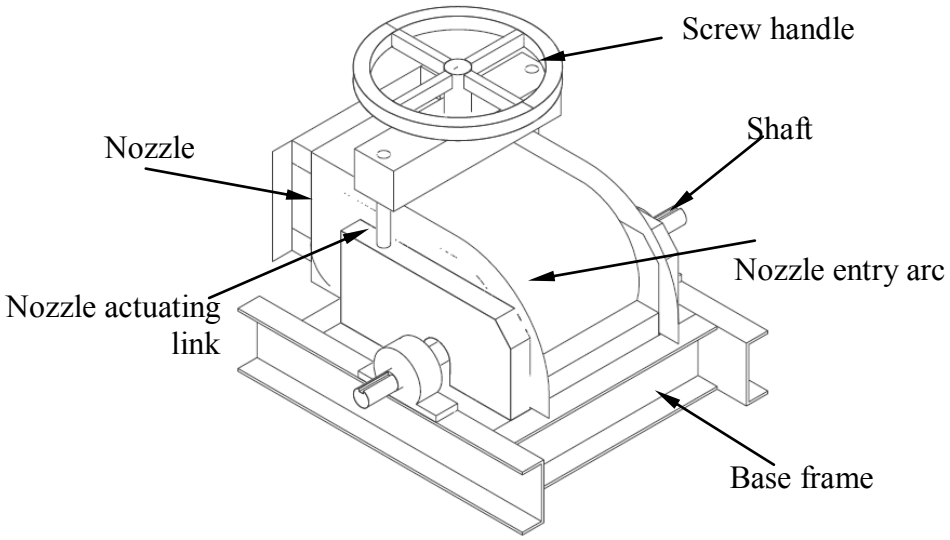

Figure 3. Pictorial representation of the model Crossflow turbine housing

Table 1. Details of the model turbine design parameters

Design parameter	Normalized expression	Value
Diameter ratio; D_1 is outside diameter of runner D_2 is the inside diameter of the runner	$\frac{D_2}{D_1}$	0.693
Angle of attack	α	16 degrees
Blade angle (outside runner periphery)	β_1	30 degrees
Blade angle (inside runner periphery)	β_2	90 degrees
Radius of the blade (r_b)	$\frac{r_b}{D_1}$	0.157
Radius from centre of the runner to the centres of where blades are drawn	$\frac{R}{D_1}$	0.378
Admission arc	φ	90 degrees
Number of blades	n_b	24
Nozzle opening	$\frac{l}{D_1}$	0.254
Nozzle width where W is the runner width	$\frac{B}{W}$	1
Radius of the nozzle entry arc	$\frac{r_{(\emptyset)}}{D_1}$	0.567

In a truly impulse turbine all of the potential energy in water is converted into kinetic energy in the jet and the entire part of the runner is exposed to atmospheric pressure. It is the kinetic energy that is converted into the turbine shaftpower. The flow in the impulse turbine does not depend on the runner speed of rotation. In a reaction turbine, both pressure energy and kinetic energy of the water are converted into shaftpower. The turbine has to be filled with water at all time during its operation. There is significant pressure difference between the inlet and outlet of the turbine. The flow through the turbine depends on the speed and pressure across the turbine.

The input power to the turbine is the hydraulic power available at the turbine inlet. The performance of the turbine is concerned with how much this hydraulic power is converted into turbine shaftpower. This is expressed in terms of its maximum efficiency (which is obtained at the designed best operating point). The performance of the turbine also concerns determining how sensitive the maximum efficiency is with respect to variations in flow and head changes. Two efficiencies are used when modeling the operation of the turbine, namely: hydraulic efficiency and turbine efficiency.

Hydraulic efficiency gives how much maximum power can be extracted from the available hydraulic power. The maximum power extracted from the water by the turbine runner is defined theoretically by the Euler's turbine equation, which assumes that there are no incidence and all other losses concerning flow through the runner. The Euler turbine equation gives power in form of flow velocities at inlet and outlet of the turbine blade spacing filled by the jets. In practice, it is extremely difficult to measure such velocities so as to calculate the hydraulic efficiency. But it is important to look at the hydraulic efficiency of the turbine because it gives asymptotic design values with which turbine design parameters can be optimized.

By applying the Euler turbine equation for power transfer analysis in the runner and using the Torricelli's theorem to relate the velocity of the jet at nozzle outlet (assumed equal to the absolute velocity) and the net head, the following maximum theoretical efficiency relation can be obtained for the Crossflow turbine:

$$\eta_h = C_v^2 \cos^2 \alpha_1 \quad (1)$$

It can also be shown that the maximum hydraulic efficiency occurs when the runner is rotating at a peripheral velocity equal to half the cosine component of the absolute velocity (velocity of the jet from the nozzle) with respect to the tangent at its entry into the first stage. The angle between the absolute velocity and the tangent (or runner periphery velocity) is known as angle of attack. This implies that if the angle of attack is small, then the Crossflow turbine periphery velocity for maximum efficiency compares well with those of Pelton and Turgo turbines whose runner peripheral velocities at maximum efficiency, are equal to half of the absolute jet velocity (for Pelton) and just less than half (0.46 to 0.47) of the absolute jet velocity for Turgo turbines [2,3].

The equation (1) is the basis for optimization of the angle of attack. As stated already in Euler turbine equation, equation (1) at assumes absence of hydraulic losses in the runner and that the jet flow is perfectly guided through the blades. To perfectly guide jet flow within the blades, the theoretical runner has to have optimum number of blades. If the blades are too few, jet flow separation may occur and for excessive number of blades, many blades may be filled with water and back pressure may occur: both conditions increase hydraulic losses and reduce efficiency. This shows that number of blades can affect the maximum efficiency levels that the turbine can achieve. Apart from affecting efficiency, blades can also have influence on the cost and structural integrity of the turbine. Too many blades will increase the cost but will ensure structural integrity.

There have been several experimental investigations, using physical Crossflow turbine models in laboratories, to determine the optimum number of blades for maximum efficiency. From the Table 2, it appears that the reported studies do not converge to a common number of blades for maximum efficiency. It can be concluded that for small-scale Crossflow turbine optimum number of runner blades used ranges typically from 15 to 35.

From equation (1), it can be seen that the smaller the angle of attack is, the better the maximum efficiency becomes. The theoretical maximum efficiency corresponds to an angle of attack of zero degrees. However, there is a practical limitation to this optimization because smaller angles of attack limit the radial flow velocity which determine amount of crossed-flow that impart torque in the second stage of the runner. The reported values for optimum angles of attack lie between 15 and 35 degrees (Table 3). However, most of turbine Crossflow turbines have been constructed with an angle of attack of 16^0 as that which was once proposed by Banki [4]. The reason may be of constructional convenience because the angle of attack of 16^0 corresponds to the blade angle of 30^0, which is relatively easy to mark-out on the disc plates on which to attach the blades.

3.2 Laboratory based determination of efficiency and performance characterisation

The practical method to describe the efficiency is to evaluate the proportion of inlet hydraulic power that has actually been extracted as shaftpower by the turbine. This is known as turbine efficiency or global efficiency. Mathematically, the turbine efficiency η_t is given by equation (2):

$$\eta_t = \frac{P_s}{P_h} = \frac{T\omega}{\rho Q\, g H_e} \quad (2)$$

where P_s shaftpower (W), P_h is the hydraulic power (W), T is shaft torque (Nm); ω is runner angular velocity (rad/s), ρ is the density of water (kg/m^3), g is the acceleration due to gravity (m/s^2), Q is the water flow rate (m^3/s) and H_e effective head (m).

Table 2. Optimum number of blades used in the experiment or number of blades used in the experiment to determine the effect of blades on efficiency by various investigator

Study Authors	Optimum number of blades used or number of blades used in the experiment to determine the effect of blades on efficiency	Remarks
Mockmore and Merryfield [4]	18	18 was determined theoretically but they used 20 in the manufacture of the model for performance testing
Varga [5]	30	
Nakase *et al*.[6]	26	
Meier [7]	28	Specifically designed as an appropriate technology under the Crossflow Turbine BYS/T1 project for the Swiss Center for Appropriate Technology
Durgin and Fay [8]	20	
Khosrowpanah *et al*. [9]	10, 15, 20	This was an experimental investigation and it was found out that 15 blade runner gave maximum efficiency than the 10 or 20 blades runners
Desai and Aziz [10]	15, 20, 25, 30	This was experimental investigation and it was found the efficiency increased with increase in number of blades. The maximum efficiency was obtained with the runner with 30 blades. It is difficult to conclude that this was the maximum number of blade for maximum efficiency because 30 blades runner was the last experiment.
Totapally and Aziz [11]	25, 30, 35, 40	This was experimental investigation and it was found the efficiency increased with increase in number of blades but showed that there is an optimum number of blades. The maximum efficiency was obtained with the runner with 35 blades. It was concluded that optimum number of blades should be within the vicinity of 35
Barglazan [12]	28	
Choi *et al*. [13]	26	
Andrade *et al*. [14]	24	
Sammartano *et al*. [15]	35	
This study	24	

Table 3. Number of blades used on optimum laboratory scale Crossflow turbine performance investigations and number of blades used in the experiment to determine the effect of number of blades on efficiency by various investigators

Study Authors	Optimum angle of attack used or angles used in the experiment to determine the effect of angle of attack on number of blades	Remarks
Mockmore and Merryfield [4]	16^0	
Nakase *et al*. [6]	15^0	
Johnson *et al*. [16]	16^0	
Durgin and Fay [8]	16^0	
Fiuzat and Akerkar [17]	16^0, 20^0, 24^0	The experiment to determine influence of angle of attack on efficiency. It was discovered that efficient increased with angle of attack: the 24^0 angle of attack gave highest efficiency. It is not possible to conclude on optimum value because 24^0 angle was the last experiment.
Khosrowpanah *et al*. [9]	16^0	
Desai and Aziz [10]	22^0, 24^0, 26^0, 28^0, 32^0	The experiment to determine influence of angle of attack on efficiency. It was concluded that optimum angle of attack was in the range of 22^0 to 24^0. This is in agreement with Fiuzat and Akerkar [17]
Barglazan [12]	15^0	
Choi *et al*. [13]	30^0	
De Andrade *et al*. [14]	16^0	
Sammartano *et al*. [15]	22^0	
This study	16^0	

The variables in equation (2) which are used to evaluate turbine efficiency can be measured in a laboratory using instruments which are described in Table 4. The effective head at inlet to the turbine can be measured through use of Bernoulli equation; the result given in the equation (3):

$$gH_e = \frac{V_1^2}{2} + \frac{P_1}{\rho} + Z \tag{3}$$

where V_1 is the velocity of water at inlet to the turbine (m/s), P_1 is the gauge in pressure (N/m^2) at point inlet and Z is the height difference (m) between the pressure transducer and the centre of the Crossflow turbine runner. The velocity V_1 can be calculated from the measured flow rate Q (m^3/s) using the continuity equation, equation (4), from knowledge of the cross-section of the pipe at inlet.

$$V_1 = \frac{Q}{A} = \frac{4Q}{\pi D^2} \tag{4}$$

where D is the diameter (m) of the pipe at inlet.
It can be seen from equation (2), that the performance of the turbine depends on several variables. It is not practical to conduct experiment for all variables to predict their effects on performance. Dimensional analysis is commonly employed to lump up variables into dimensionless variables. These dimensionless groups can then be plotted so as to show the variation of one with each the other. The performance

relationships in form of graphs can then be applicable to any such Crossflow turbines that are dynamically and geometrically similar.

From experience, neglecting scaling effects, the independent variables that determine the performance of the turbine are physical variable (torque T), dynamic property (specific head gH_e), dynamic property (Q), flow property (density ρ), and geometry of the runner (runner diameter D) and kinetic property (runner speed n). There are six independent variables and three primary dimensions of mass, length and time; so three dimensionless can be formed using Buckingham Pi Theorem. Using $(gH_e), \rho$ and D as the repeating variables, the dimensionless groups formed are: $\pi_1 = \frac{Q}{D^2\sqrt{gH_e}}$; $\pi_2 = \frac{nD}{\sqrt{gH_e}}$; $\pi_3 = \frac{T}{\rho D^3 gH_e}$.

These dimensionless groups are also referred to as reduced quantitative. π_1 is the reduced flow rate (Q_{ED}), π_2 is the reduced speed (n_{ED}) and π_3 is the reduced torque (T_{ED}). These are the dimensionless groups are among those outlined in the International Electrotechnical Commission (IEC) Standard 60193 on testing of hydraulic turbine models [18]. The plots of these dimensionless groups characterize the performance of the Crossflow turbine, as it has been applied in this experimental study.

3.3 Theoretical torque transfer in the two stages: Using Euler's turbine equation

The other objective of this work is to characterize the two stage power transfer in the runner. The theory behind analytical and experimental approach will be looked at in this section of the paper.

Power transfer is the result of the resultant torque exerted on the blades in both stages as a result of change of angular momentum of the jet.

Due to complex action of the Crossflow turbine, the theoretical torque transfer analysis can be possible if assumptions are made. These assumptions are there are no losses incurred such as incidence, shocks and friction.

Consider the flow through the runner passing through first stage as schematically shown in Figure 4 (inlet designated 1 and outlet designated 2) and second stage (inlet designated 3 and outlet designated 4). If Newton Second Law of Motion is applied to a mass of water flowing with an infinitesimal velocity ($d\vec{C}$) in a unit time in the direction of the velocity vector, then an infinitesimal force ($d\vec{F} = \rho Q d\vec{C}$) is generated by the fluid. The infinitesimal reaction force ($d\vec{R}$) on the blade is equal and opposite of this force, according to Newton Third Law of Motion. Therefore, the forces on the runner in the first stage ($R_{1\to2}$) and second stage ($R_{3\to4}$) are as follows:

$$R_{1\to2} = -\int_1^2 \rho Q d\vec{C} = \rho Q(\vec{C}_1 - \vec{C}_2) \tag{5}$$

$$R_{3\to4} = -\int_3^4 \rho Q d\vec{v} = \rho Q(\vec{C}_3 - \vec{C}_4) \tag{6}$$

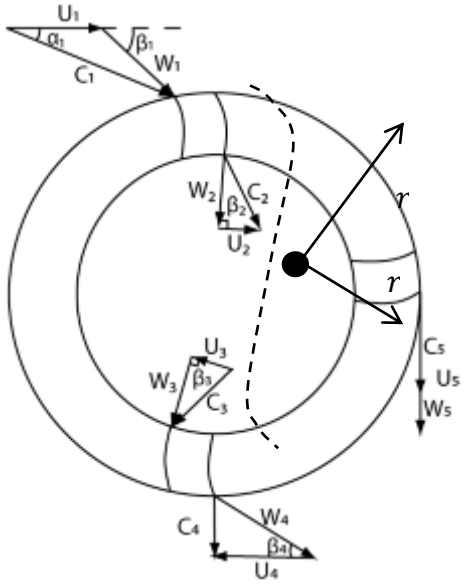

Figure 4. Flow path and velocity triangles in a Crossflow turbine runner

To generate power, it is important to calculate torque due to these forces about the axis of rotation of the runner. When using the equations (5) and (6), the absolute velocity vectors can also be expressed in terms of their orthogonal components, tangential component (C_u) and radial components (C_r). The velocity vector responsible for torque production is the tangential component also known as velocity of whirl. The radial component does not produce torque because its line of action passes through the axis of rotation. Therefore, taking multiplication of the force due to change in whirl velocity and its corresponding radius:

$$T_{1\to2} = \rho Q\left(\vec{C}_{u1} r_1 - \vec{C}_{u2} r_2\right) \tag{7}$$

$$T_{3\to4} = \rho Q\left(\vec{C}_{u3} r_3 - \vec{C}_{u4} r_4\right) \tag{8}$$

The ratio of power transfer during both stages can be given as:

$$\frac{T_{1\to2}\omega}{T_{3\to4}\omega} = \frac{\vec{C}_{u1} r_1 - \vec{C}_{u2} r_2}{\vec{C}_{u3} r_3 - \vec{C}_{u4} r_4} \tag{9}$$

where ω (rad/s) is the angular velocity of the runner.
From geometry of the velocity triangles and noting that the water jet must leave the first stage with radial relative velocity and enter the second stage in radial direction:

$$\vec{C}_{u1} = U_1 + W_1 \cos\beta_1 \tag{10}$$

$$\vec{C}_{u2} = U_2 = \vec{C}_{u3} \text{ and } \vec{C}_{u4} = C_4 \cos\alpha_4 \tag{11}$$

It can be shown from design optimization that for maximum efficiency, that the flow must leave the second stage without whirl, therefore:

$$\vec{C}_{u4} = 0 \tag{12}$$

Further, it can be shown from optimisation of the blade angle with respect to runner periphery speed that for maximum efficiency,

$$U_1 = W_1 \tag{13}$$

Angular velocity of the runner ω is constant,

$$U_1 = \omega r_1 \text{ and } U_2 = \omega r_2 \tag{14}$$

$$\vec{C}_{u1} = U_1(1 + \cos\beta_1) = \omega r_1(1 + \cos\beta_1) \tag{15}$$

Substituting terms in equation (9):

$$\frac{T_{1\to2}}{T_{3\to4}} = \frac{\omega r_1(1+\cos\beta_1)\times r_1 - \omega r_2 \times r_2}{\omega r_2 \times r_2} \tag{16}$$

$$\therefore \frac{T_{1\to2}}{T_{3\to4}} = \left(\frac{r_1}{r_2}\right)^2 (1 + \cos\beta_1) - 1 \tag{17}$$

The equation (17) shows that, for an optimised design, the ratio of power transfer in the two stages theoretically depends on the size of the runner and the blade angle. It can be seen from the equation that it is the first stage always contribute more power than second stage.
For the simple Crossflow turbine runner under, using the design parameters laid down in Table 1.

$$\frac{T_{1\to2}}{T_{3\to4}} = \left(\frac{1}{0.693}\right)^2 (1+\cos 30^0) - 1 = 2.89$$

Therefore percentage contribution of each stage to total torque production

$$\%T_{1\to2} = \frac{T_{1\to2}}{T_{3\to4}+T_{1\to2}} = \frac{2.89T_{3\to4}}{3.289T_{3\to4}} = 0.743$$

Similarly,

$$\%T_{3\to4} = \frac{T_{3\to4}}{T_{3\to4}+T_{1\to2}} = \frac{1T_{3\to4}}{3.289T_{3\to4}} = 0.257$$

Therefore, theoretically, the first stage contribute 74.3% to the total torque (or power) production while the second stage produce the remaining, 25.7%.

3.4 Two stage power transfer using impulse principle: development of theory behind use of strain gauge

For a Crossflow turbine, the runner blades are subjected to intermittent forces which can be described theoretically by impulse principle. The Newton second law of motion can be applied to calculate net force ($\vec{F}_{net}$) exerted by an identifiable mass (m) of water jet (system) impinging the blade:

$$\vec{F}_{net} = m\frac{d\vec{C}}{dt} = \frac{d}{dt}(m\vec{C}) \tag{18}$$

In classical mechanics, the impulse of a force is defined as the product of the average force and the time it is exerted. In this case, considering the Newton second law equation (18), the change in momentum is equal to the impulse of the net force:

$$J = \int_{t_1}^{t_2} \vec{F}_{net}\, dt = \vec{F}_{av}(t_2 - t_1) \tag{19}$$

$$\therefore \vec{F}_{av} = \frac{\int_{t_1}^{t_2} \vec{F}_{net}\, dt}{t_2 - t_1} \tag{20}$$

where J is the impulse (Ns), $\vec{F}_{av}$ is the average force (N) that gives the same impulse as the actual force in the same interval of time, $(t_2 - t_1)$, (s). If the relationship between the net force and time is established whether from theory or experiment, then it is possible to calculate the average force acting on the blade in first stage and second stage by integrating the areas under the curve and noting the time intervals, as illustrated is Figure 5. Once the average forces are calculated, then it is possible to calculate torque and determine the power transfer characteristics in the stages.

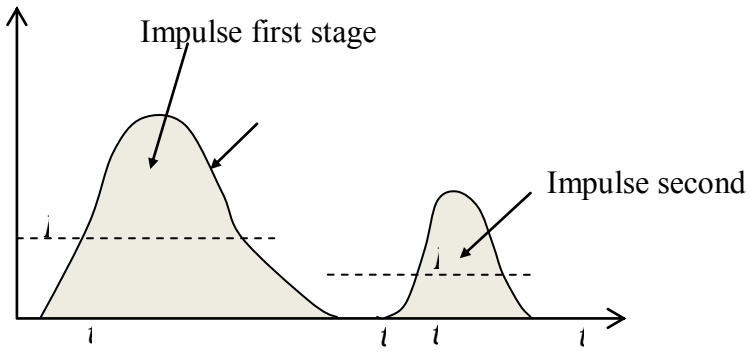

Figure 5. Illustration of impulse force principle

In this experimental investigation, strain gauge will be used to calculate the intermittent net force $\vec{F}_{net}$ with time. The methodology is explained in the 'Methodology and instrumentation' section. In this section, the theory using the strain gauge in characterizing torque in the two stages is presented.
Strain gauge is a transducer that measures change in dimension (called strain) of a body when force is applied to cause deformation. The most common types of strain gauges consist of an insulating flexible backing which supports a metallic foil which is attached to the body (Figure 6). When the object is deformed due to the applied force, the foil is deformed also, causing its electrical resistance to change. The change in resistance is proportional to the change in deformation of the foil and hence the applied force. Using Ohms law, the change in resistance of the foil can be related to change in voltage which can be measured usually by employing a Wheatstone bridge circuit. The strain gauge therefore, has to be attached to the object by a suitable adhesive such as cyanoacrylate.

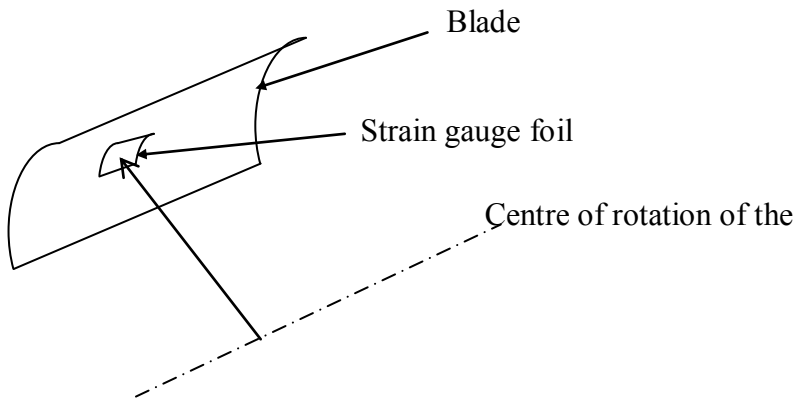

Figure 6. Illustration of blade and strain gain gauge foil

The strain gauge can also be used to measure force and stress on the object such as the blade that is exposed to intermittent force (such as in this experimental investigation). If the deformation due to applied force on the blade is assumed elastic, then Hooke's Law can be applied:

$$\vec{F}_{net} = k\delta l \tag{21}$$

where k is the constant (Nm^{-1}) which depend on the property of the foil, δl is the change in dimension (m).

From the definition of strain:

$$\varepsilon = \frac{\delta l}{L} \tag{22}$$

where ε is the strain, L is the original dimension (m), the length of the wire foil in this case.

$$\vec{F}_{net} = k\varepsilon L \tag{23}$$

Torque due to this force on the blade at a radius r from the centre of the runner rotation,

$$\vec{T}_{net} = \vec{F}_{net} \times r = k\varepsilon Lr \tag{24}$$

$$\vec{T}_{net} = (kLr)\varepsilon \tag{25}$$

$$\vec{T}_{net} = k_0\varepsilon \tag{26}$$

The original length of the wire, L, radius if the runner, r, and k are all constants which imply that the torque can be measured in terms of strain ε. The strain, which will be measured in terms of voltage signal, will vary with the magnitude of the net force on the blade which is function of time. The torque in

equation (26) will be measured in terms of voltage. To measure this torque, therefore, the overall constant ($k_0 = kLr$) must be evaluated by calibrating the strain gauge. However, for this experimental investigation, it is not necessary since only a ratio of torque transfer in two stages will be analysed.
The average torque on the blade in the two stages blade can be calculated by integrating the area below the curve of torque (voltage in this case) against time and noting the time duration (t_2-t_1) between the stages using the equation (20) as follows:

$$\vec{T}_{av} = \frac{\int_{t_1}^{t_2} \vec{T}_{net}\, dt}{t_2 - t_1} \tag{27}$$

Or

$$V_{av} = \frac{\int_{t_1}^{t_2} V dt}{t_2 - t_1} \tag{28}$$

where V_{av} (volts) is the average voltage, V (volts) is the voltage at time t (s).

4. Methodology

This is an experimental investigation on the simplified Crossflow turbine model that was manufactured based on the normalized parameters given in Table 1. The model was installed for testing in the Waterpower Laboratory of the Norwegian University of Science and Technology in 2013. The Waterpower Laboratory has two loops that can be used for testing different types of turbines: the free surface loop and the pressurized tank loop. This experiment utilized the free surface loop which has a maximum level of 14 m between levels of water in the reservoir in the basement of the laboratory and the water free surface level in the upper two open tanks located in the uppermost floor of the laboratory. There are two speed variable centrifugal pumps that pump water from the reservoir either to pressurized tank or to the open tanks. The flow of water in the circuits to test rigs is controlled by valves and the control is automated using LabVIEW program.

4.1 Experiment layout and instrumentation description

The layout showing the free surface loop system and the instrumentation for this experiment is shown schematically in Figure 7.

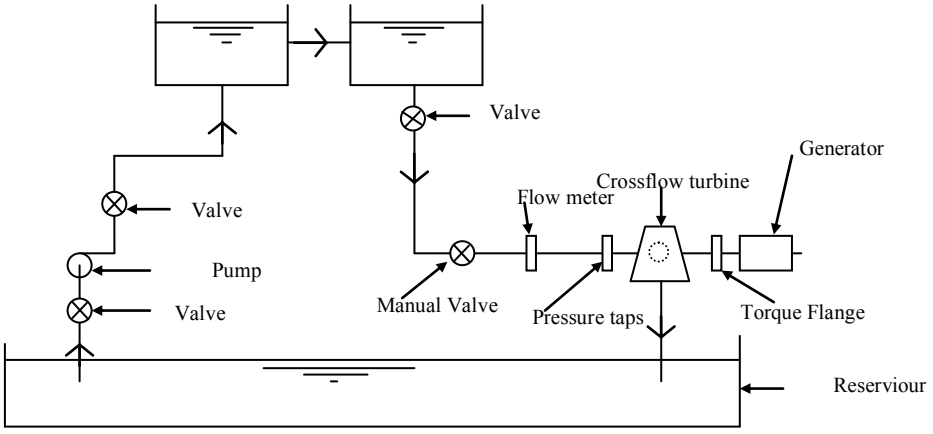

Figure 7. Experiment layout, water flow circuit and instrument arrangements

Data logging from the measurement instruments and control of experiment was done using the labVIEW program installed into the data logging computer. The labVIEW program requires input signals to be in form of voltage. Because of this, measurement instruments were calibrated using the standard facilities and tools in the laboratory to determine the constants of the relationships (linearised graphs) between the measured quantities and the resulting voltage signal output. The other reason for instrument calibration was to evaluate the uncertainties so as to account for systematic errors during measurement. The instrument calibration in the Waterpower Laboratory is performed according to the procedures outlined in IEC 60193 [18]. Description of measuring instruments is given in Table 4.

Table 4. Details of measuring instruments

Instrument Description	Quantity to measure	Range	Uncertainty (%)
Pressure Transducer manufactured by Fuji Electric France S.A	Gauge pressure at turbine inlet	± 2000 kPa	± 0.25
Torque Flange, T10F/FS model manufactured by Baldwin Messtechnik GmbH	Torque at turbine output shaft	± 1000 Nm	± 0.09
Electromagnetic flow meter, Krohne IF 4000 manufactured by Krohne Marshall Private Ltd.	Water flow rate into the turbine	0 – 1 m^3/s	± 0.12
Tachometer (in-built in the Torque Flange)	Rotation speed of the turbine	0-12000	± 0.63
Strain gauge, HBM model LY6	Strain in the blades	350 Ω nominal resistance	± 0.35
ST-500 Wireless transmitter manufactured by Wireless Link Digital Telemetry System	To send strain voltage gauge signal to logging computer,		n/a

Water flow in the pipe to the turbine is measured using the electromagnetic flow meter IF 4000. The meter is excited with an external voltage to create a magnetic field. When water, a conductive liquid (water in this experiment), flows through the magnetic field, voltage is induced. This voltage is proportional to the velocity of the flow and hence flow rate. The voltage is measured by two stainless steel electrodes mounted opposite each other inside the metering pipe. The two electrodes are connected to an electronic input circuitry which processes the voltage signal.

The pressure is measured by the pressure transducer. Four pressure taps, equally spaced, supported by a ring, taps water flow from the pipe and conveys it to the pressure transducer. The transducer has a sensor that generates voltage signal in response to pressure force applied against the sensing element. The sensor does not come into contact with the flow water, but is protected from it by the use of isolating diaphragm and a fill fluid. The measurement of pressure in this way is based on Pascal's Law which states that whenever an external pressure is applied to confined fluid at rest, the pressure is increased at every point in the fluid by the amount of that external pressure. The pressure taps are connected to the piping in such a way that the flow pressure is exerted against the isolation diaphragm(s). According to the Pascal's Law, the fill fluid inside the primary element will reach the same pressure as that applied against the isolation diaphragm. The fill fluid hydraulically conveys this pressure to the sensor, which in turn produces a voltage signal.

Torque on the turbine output shaft is measured by the torque flange using strain gauge using the principle that the resulting strain in the shaft is proportional to the applied torque that is generated. The strain gauges are bounded to the torque flange. The strain is converted into corresponding change in resistance of the strain gauge wire. Through a four-arm Wheatstone Bridge circuit, the voltage is generated proportional to the strain hence torque generated. The voltage signal transfer between the rotating torque flange shaft and the stationary housing is accomplished by means of rotary transformer.

The turbine rotational speed is measured by the tachometer which is in-built in the torque flange. The speed sensor in the tachometer works on the principle of magneto-resistive effect of a current carrying conductor in the presence of an external magnetic field. Rotational speed measurement using magneto-resistive sensors is achieved by counting ferromagnetic marks, such as teeth of a passive gear wheel or the number of magnetic elements of magnetized ring. In this tachometer, the gear is attached to the rotating shaft. A magnet attached to one side causes a variation in the magnetic field that is sensed by the sensor, and the variation is converted to a square wave voltage signal where each edge corresponds to one edge of the toothed wheel. The time between two or more edges is then registered and converted into angular speed.

All the voltage signals generated by the measuring instruments are transmitted by cables via the data acquisition card to the data logging computer (refer to Figure 8) using specific channels.
A LabVIEW program was written to log in signals and process voltage signals into corresponding real values of measured variables and process the performance parameters of the turbine from the measured variables. The program calculates input hydraulic power, shaft power, torque, efficiency, reduced speed, reduced flow rate, reduced torque and effective head for the turbine.

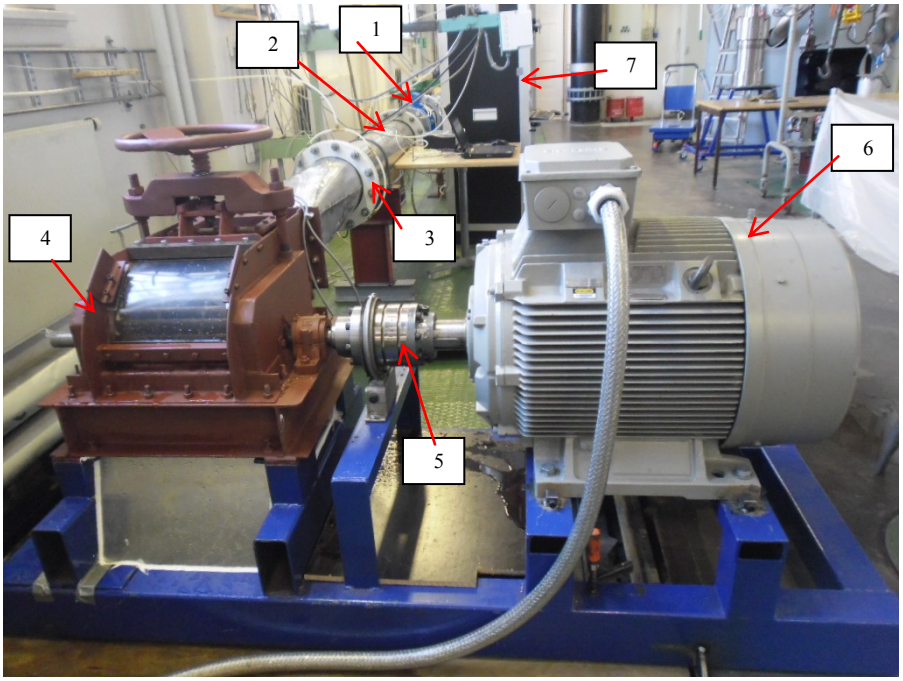

Key:
1 = Electromagnetic flow meter

2= Pipe carrying water to turbine

3= A ring supporting 4 equally spaced pressure taps from where water is tapped to the pressure transducer through tubes.

4 = Assembled turbine

5 = Torque flange with an in-built tachometer

6= Variable speed generator

7 = Data processing computer compartment

Figure 8. Picture showing part of the test set-up and arrangement of measuring instruments

4.2 Test procedures

4.2.1 Procedure for performance characterization

Firstly, the required loop from the free surface tanks to the Crossflow turbine test rig was identified by opening the appropriate valves on the Programmable Logic Controller (PLC). Then, using the PLC, water is pump into the tanks from the lower reservoir. The maximum free surface level in the tanks is controlled by a valve such that there is no overflow. In the event of an overflow, there is an overflow pipe to the lower reservoir.
The head to the turbine was controlled by the pump speed as well as by opening and closing of the manual valve (through head loss in the valve). Pump speed was controlled remotely through a LabVIEW on the PLC. The flow into the turbine runner is controlled by the valve opening which has five marked opening positions; from 100% to 0 (representing a 20% difference between the markings).
At a particular head, the valve was set to a marked amount of opening (starting with 100%) and at these two settings being constant, the experiment was run at different speeds, starting with 100 rpm to 700 rpm with an increase of 50 rpm. At the same head, the nozzle was set to a marked amount of opening of 80% and the experiment was run for different speed as at first. The same experiment procedure was followed for all the marked amount of nozzle openings at that particular head. Experiments were conducted at heads of 3m, 5m, 7m and 10m. Head of more than 10m was not possible because of the generator mechanical problems that resulted. The measured data were logged into the logging computer by running the LabVIEW program. The calculated output data was exported from labVIEW to Excel for further processing.

4.2.2 Procedure for stage torque transfer characterization and strain signal data processing

The strain gauge was glued to the suction side of the blade using silicon adhesives. The blade glued with strain gauge was attached to one of the end discs of the runner. The signal from the strain gauge was transmitted to the wireless transmitter was positioned at the end of the shaft. The transmitter was

connected to the strain gauge by a wire. The signal was sent to the receiver by the wireless transmitter. A labVIEW program was written to log data from the receiver with a sample rate of 4000 per second.
It was necessary to identify the two stages in the signal curve to perform integration so as to calculate ratio of torques produced in the stages, as outlined in the theory. This was done by identifying positions of peaks in the signal plot and the times at which the peaks start and terminate.
The original signal, as observed from the LabVIEW program, repeated itself but contained significant levels of noise which needed to be filtered without affecting the original shape of the signal. The signal was filtered using a low pass filter in the LabVIEW program using a filtering frequency of 100 Hz that was found to be suitable after a trial of several frequencies (for example, Figure 9a). However, the signal at 20% valve opening contained excessive levels of noise such that even after filtering out with a frequency of 100 Hz, significant amount of noise was still present. This signal was further filtered with a frequency of 30 Hz which was found suitable. This filtering of the signal at lower frequency made the original signal lose its shape (Figure 9b). The 20% valve opening signal was subsequently excluded from the experiment because it was judged that a lot of information has been lost through filtering.

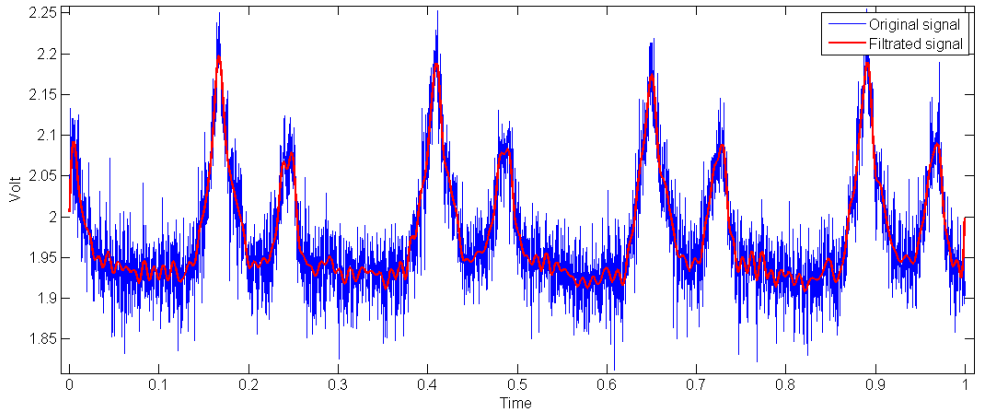

(a)

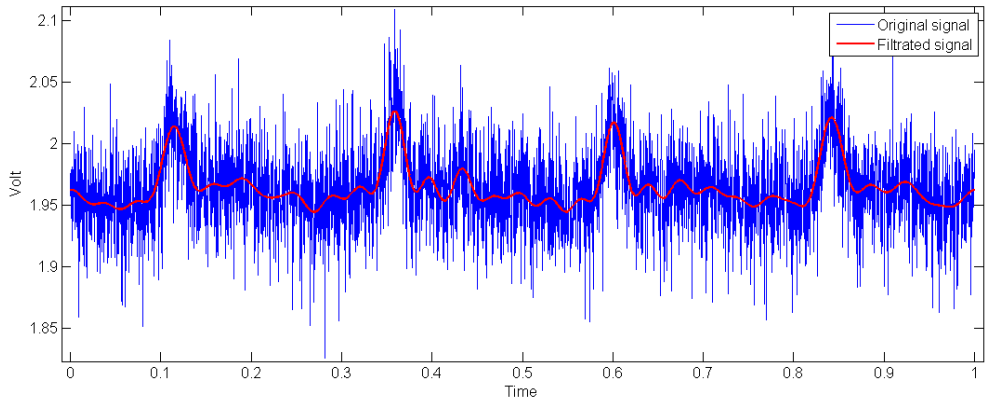

(b)

Figure 9. (a) Filtering at 80% valve opening (clearly identified peaks); (b) Poor signal at 20%. It was excluded from the experiment analysis

A Matlab program was coded to identify positions of peaks and the times at which the peaks start and terminate. The program plotted filtrated signal against time. The average length of peaks and times between the start and termination points of peaks were calculated from the program. The peak points were manually selected using the Data Cursor Tool.
A second LabVIEW program was written to integrate areas of the peaks with input from the Matlab program. The values calculated in Matlab and LabView will be further processed in a spreadsheet calculating the amount of transferred torque during the two stages in percent.
Since the magnitude of voltage signal signify presence of torque which is only generated when the jet flows through the blade spaces, it is possible to calculate the portion of the runner that is being used for torque production. This was done by calculating the angle ψ, known as the runner utilisation angle,

between the water entering the first stage and leaving the second was calculated. This is done by taking note of the time under the 'peaks' and the periodic time for the signal from the Matlab program.
The relative torque transfer characterization in the stages was carried out at best efficiency point (5m, 80% valve opening and 350 rpm - corresponding to 13.4 reduced speed) so as to compare with the theoretically calculated value for maximum efficiency. It was also designed to evaluate the manner of torque transfer outside the best efficiency point. However, the test at more than 350 rpm rotational speed caused mechanical problems to the strain gauge and the experiment was not carried out. Therefore, the strain gauge experiment was carried out at 250 rpm and 350 rpm. At each experiment point, tests were conducted three-times so as to compare and ensure that correct data is obtained.

5. Results and discussion

5.1 Turbine performance characterization results and discussion

The maximum efficiencies at each of the nozzle position, head and the corresponding reduced speeds are given in Table 5.

Table 5. Maximum efficiency of Crossflow turbine at different heads and positions of nozzle opening

Head	Maximum efficiency at 20% nozzle opening (N_{ed})	Maximum efficiency at 40% nozzle opening (N_{ed})	Maximum efficiency at 60% nozzle opening (N_{ed})	Maximum efficiency at 80% nozzle opening (N_{ed})	Maximum efficiency at 100% nozzle opening (N_{ed})
3m	0.44 (11.6)	0.59(11.6)	0.635(11.6)	0.668 (12.4)	0.647 (13.2)
5m	0.52 (10.8)	0.65(11.6)	0.73(13.2)	0.79 (13.4)	0.768 (14)
7m	0.51 (11.2)	0.63(11.2)	0.73(12)	0.765 (12.8)	0.756 (13.6)
10m	0.51 (11.2)	0.629 (11.2)	0.69 (12)	0.736 (12.8)	0.729 (13.6)

From Table 5, the following performance characteristics for the simplified Crossflow under study can be drawn:

- The turbine maximum efficiency for conditions understudy is 79% at a head of 5m, reduced speed of 13.4 and valve opening of 80%. This is the best efficiency point (bep) of the turbine.

For a small simplified Crossflow turbine this measured efficiency of 79% is relatively high. However to improve the efficiency further, it is important to study the flow pattern and identify other areas for further improvement. Desai and Aziz [10], in the parametric study of the Crossflow turbine, found out that it is possible to achieve a measured efficiency of upto 88% with correct configurations of nozzle and runner. The measured best efficiency in this experiment compares favorably with the average efficiency of 80% for small scale Crossflow turbine manufactured by Ossberger GmbH + Co located in Bavaria, Germany [19]. The results also compare well with those obtained by other investigators as shown in Table 6.

Table 6. Some Crossflow experimental studies and maximum efficiency levels attained

Investigators	Maximum efficiency (%)
Mockmore and Merryfield [4]	68
Nakase *et al.* [6]	82
Johnson *et al.* [16]	80
Durgin and Fay [8]	66
Khosrowpanah [20]	80
Hothersall [21]	75
Fiuzat and Akerkar [1]	89
Ott and Chappel [22]	79
Desai and Aziz [10]	88
Olgun [23]	72
This study	79

- From the head of 5m, the maximum efficiency at all of the nozzle opening positions reduces with increase in head.

This performance phenomenon can be described by firstly looking at the turbine losses in the runner. There is no standard to characterize losses in the Crossflow turbine runner specifically. Therefore, the general international standard on performance evaluation of turbines can be used. According to IEC 60193 [18], the losses in the turbine comprise of fluid friction, hydraulic, leakage and shaft bearing losses. The friction losses depend on the magnitude of the relative velocity in the blades, as can be seen from Darcy-Weisbach friction head loss equation:

$$h_f = f\frac{L_c}{D_c}\frac{W^2}{2g} \tag{29}$$

where h_f (m) is the head loss due to friction, f is the friction factor, L_c (m) is the characteristic length, D_c (m) is the characteristic diameter, W (ms^{-1}) is the relative velocity and g (ms^{-2}) is the acceleration due to gravity. It can further be seen that the relative velocity is the vector difference between absolute velocity jet velocity and runner tangential velocity at inlet:

$$\vec{W} = \vec{C} - \vec{U} \tag{30}$$

When the head increases, the jet velocity C increases. At a particular maximum turbine rotational speed, the tangential velocity U at the inlet is constant and thus it can be seen that the relative velocity W increases as the head increases. Therefore, it can be further seen from Darcy-Weibach equation that the losses in the turbine increase as head increases. This contributes to reduction in efficiency as head is increased.

The hydraulic losses, according to IEC 60193 [18], can collectively be described as those losses that occur when the direction of relative velocity does not correspond with the blade angle when the jet enters the first and second stages. This mismatch can cause jet separation, jet shock on the blade edges and flow spreading to other blades, flow phenomena which are all associated with energy losses. In other turbines, these losses have been known to depend partly on absolute velocity and hence on head across the turbine. Therefore, it can be expected that as head increases with hydraulic losses from the best efficiency point. These phenomena can be explained qualitatively that a great amount of jet splashing and foam was observed in the runner when the experiment was run at higher heads. A standard qualitative and quantitative characterization of flow field in the runner can be achieved by CFD analysis.

The main leakage in the simple Crossflow turbine understudy is between the gap that is there between end of the top cover and the runner. The leakage between end sides of the runner and housing is relatively negligible because the flow in the runner is mainly radial. Again, as with the hydraulic losses, the leakage loss increases with net head across the turbine. For a pure impulse turbine, leakage is not a problem because the flow in the runner is essentially at atmospheric pressure. However, when the Crossflow turbine operates with a degree of reaction in the second stage, then leakage can be a significant component of turbine loss.

- Efficiency drops with reduction in valve opening at all heads. It is observed that when the turbine less than 80% of the valve opening, the efficiency decreases rapidly with a reduction in valve opening.

This observation will be discussed when discussing the 'reaction' behavior of the Crossflow turbine and torque transfer characterization.

The sensitivity of turbine performance away from the best performance at the tested heads is shown in Figure 10 and the following trends are observed:

- At all tested heads, except 3m, the maximum efficiency is still above 50% even when the flow is one-quarter of the best efficiency flow, i,e $0.25Q_{bep}$, (20% nozzle opening flow = 0.25 flow of 80% nozzle opening flow).
- When the flow is $0.5Q_{bep}$ to $1.2\ Q_{bep}$, the maximum efficiency is equal and above 65%. This indicates that the simplified Crossflow understudy is able to operate optimally in varied flow conditions.
- The optimum efficiencies (above 70%) at 5m head and 80% valve opening was maintained over a wide range of speeds: from reduced speed of nearly 10 to 18. Such flexibilities have been observed in other performance characterization such as those studied by Mockmore and Merryfield [4].

The characterization of the efficiency for all the heads, rotational speeds and nozzle openings is given in form of performance graphs, Figures 11 to 14.

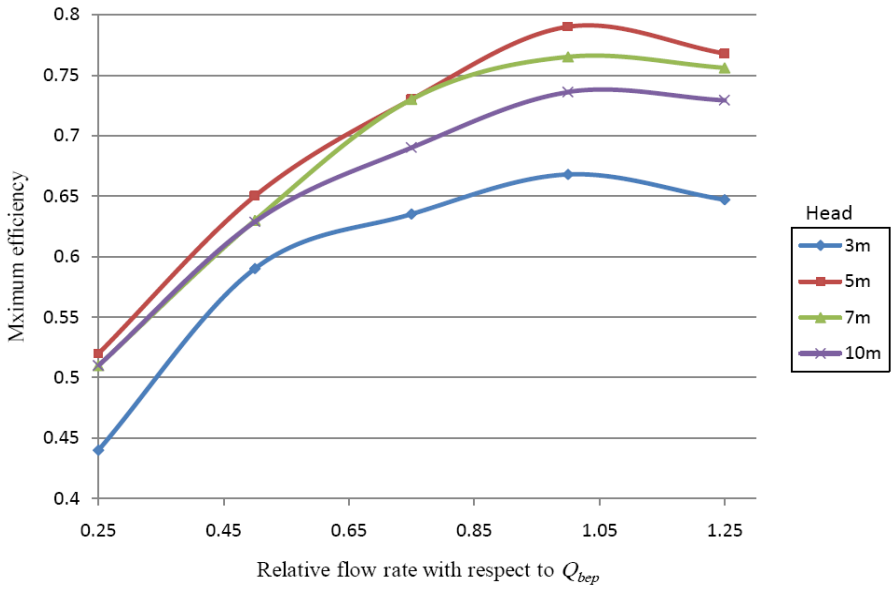

Figure 10. Performance characteristics of the simplified Crossflow turbine with respect to changes in best efficiency flow rate

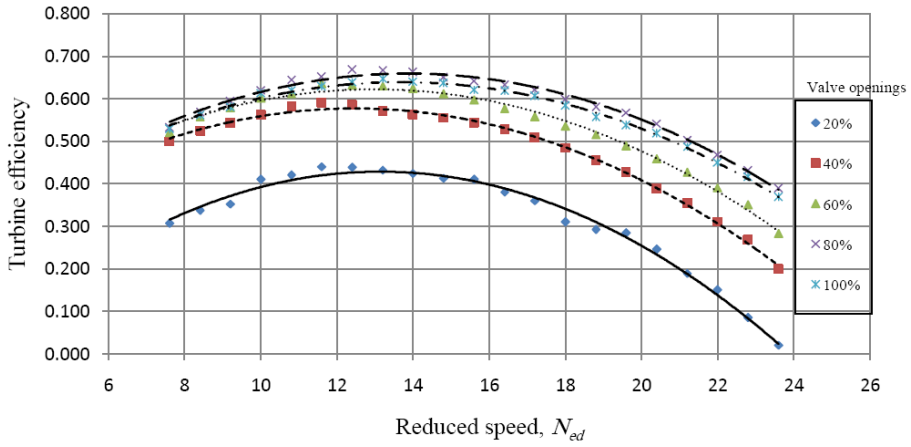

Figure 11. Turbine performance at 3m head

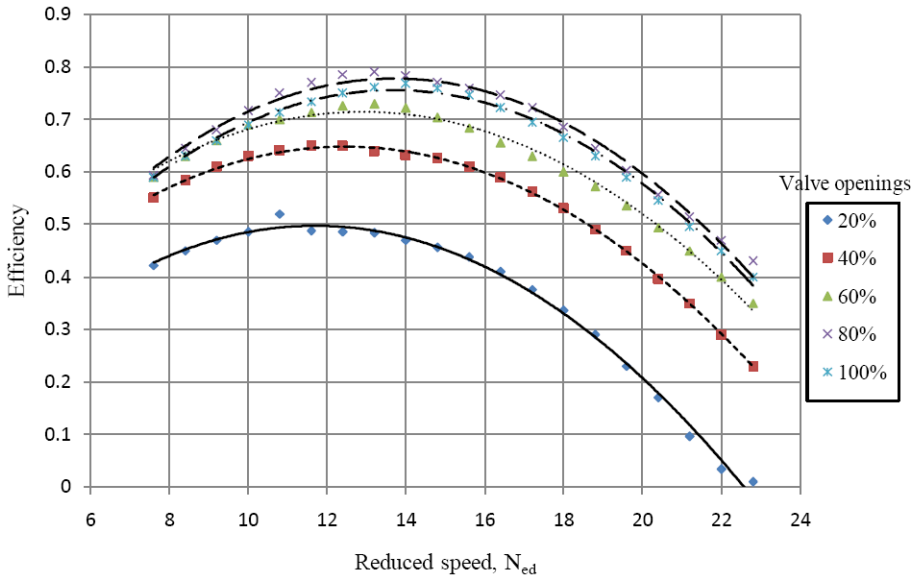

Figure 12. Turbine performance at 5m head

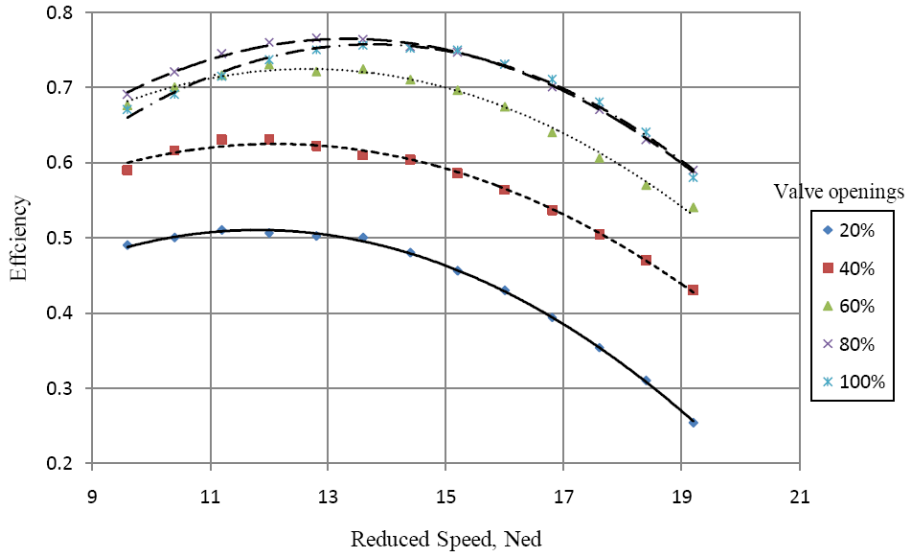

Figure 13. Turbine performance at 7m head

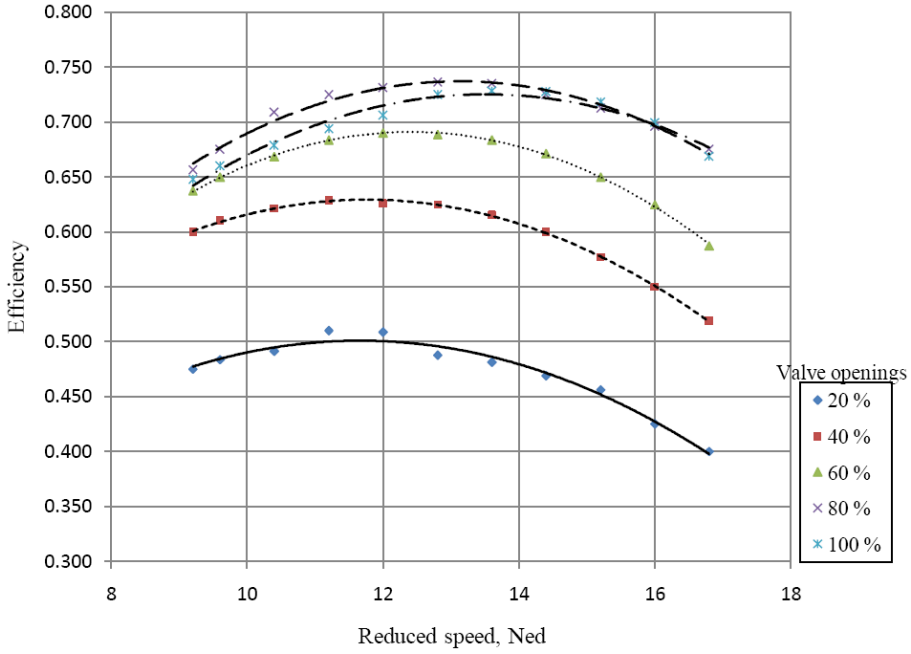

Figure 14. Turbine performance at 10 m head

- From the Figures 11 to 14, it can be seen that at each head and particular valve opening, the efficiency is a function of rotational speed of the runner. The efficiency increases with the speed upto a peak (best efficiency point for that valve opening) and then afterwards, reduces with speed.

These observations are in agreement with the Euler turbine equation: efficiency also depends on the speed of runner. When the turbine rotational speed changes from that at design point, the runner peripheral velocity becomes different from the design value. It can easily be comprehended by examining the velocity triangles that the angle between the relative velocity and runner tangential velocity at inlet is not equal to the design blade angle; as such the jet hits the inside of the blade causing incidence losses and flow separation. These losses increase with magnitude of the velocity that is deviated from the best efficiency point.

5.2 Reaction behavior of the Crossflow turbine

Figure 15 shows the relationship between flow and speed of the turbine. It can be seen from the figure, that at nozzle openings of 20%, 40% and 60%, the reduced flow (Q_{ed}) is almost constant with reduced

velocity (N_{ed}) implying that the flow rate is independent of the rotational speed of the runner. This shows that the energy transfer in the runner is due to impulse force only and not due to pressure. This performance behavior is typical for pure impulse turbines like Pelton Wheel and Turgo.
It can further be seen from Figure 15 that the Q_{ed} versus N_{ed} relationship is becoming more of 'a curve' at 80% valve opening and the 'curve' relationship is pronounced at 100% valve opening. This shows that at larger nozzle openings, the turbine exhibits some reaction characteristics because the flow through the turbine reduces with an increase in runner speed. This performance characteristic is observed with high head Francis turbines. This may be due to the fact that at large valve openings, the jet covers a bigger proportion of the first stage, therefore, flow passes through many blade spaces. The increase in blade area of contact with the flow increases the contribution of pressure energy transfer. Again, with the current design where the nozzle follows the runner housing closely, a nozzle entry arc is likely to impart a positive pressure to the flow at entry to the first stage, as already stated. However, since the flow enters the second stage passing through the empty space, the second stage is likely to operate without reaction and thus, the observation of reaction characteristics may be limited to the first stage only.
The results show that for this simplified Crossflow turbine, the maximum efficiencies are obtained when the turbine operates with a degree of reaction. This means that the area between the runner and the nozzle entry arc should be completely filled with water. The jet must enter the runner close to the nozzle outlet.

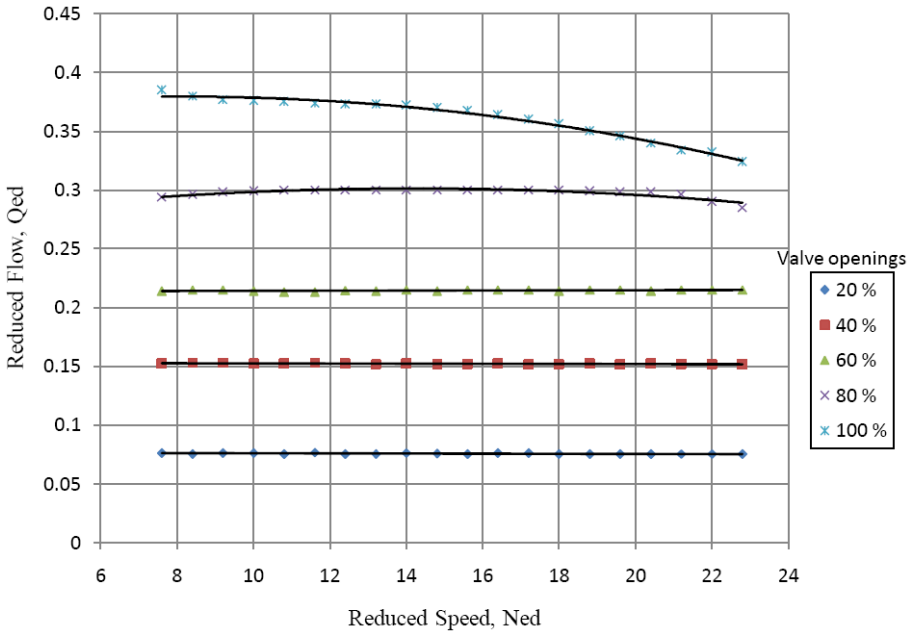

Figure 15. Performance characteristics of the crossflow turbine in form of reduced flow against reduced speed at 5m

Figure 16 shows a plot of torque as a function of runner speed at all valve openings. It can be seen from Figure 16 that for valve openings of 20%, 40% and 60%, the reduced torque varies linearly with the reduced speed. At openings of 80% and 100%, the parabolic relationship describes the relation between the reduced torque and reduced speed. This performance characteristic again shows that at small valve openings (20% to 60%), the turbine operates as a pure impulse turbine.
In a pure impulse turbine, the flow rate into the runner is does not depend on runner speed, as stated already. The absolute velocity, which is equal to the velocity of the jet is considered constant for the given head. As a result, it can be shown using the Euler's turbine equation that the torque across the turbine is expressed by:

$$T(U) = A - BU \tag{31}$$

where A is the torque (Nm), a constant that can be obtained when by braking the runner in during operation. B is another constant which is the moment of mass flow rate at a mean radius of the turbine blade relative to the centre of the runner.

In terms of reduced quantities, equation (31) can be written as:

$$T_{ed} = a - bN_{ed} \tag{32}$$

The reduced torque against reduced speed correlation equations in Figure 16 models the torque behavior for valve openings relatively correctly as in equation (32) as evidenced by the coefficient of determinations of close to 1.

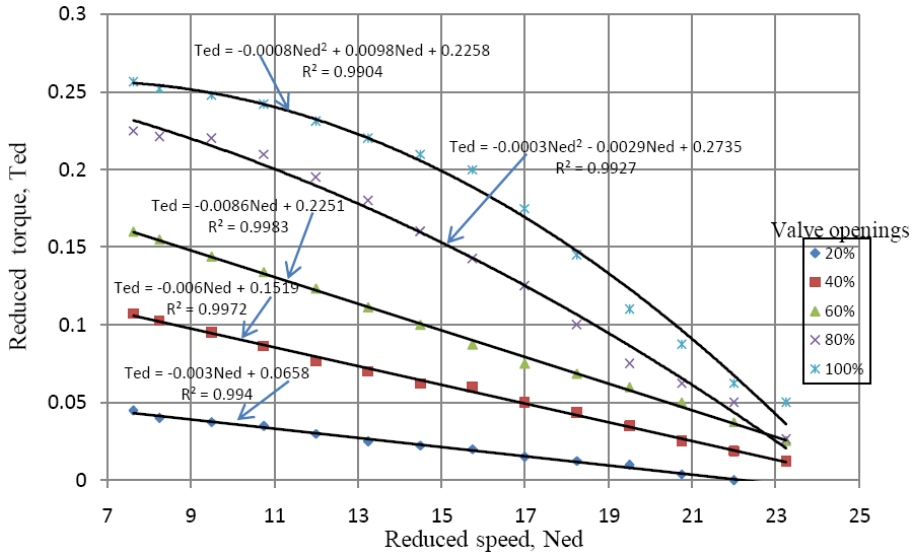

Figure 16. Reduced torque versus reduced speed at 5m

5.3 Torque transfer characterization in the runner

The theoretical analysis in the section on 'theory' showed that the first and second stages respectively contribute 74.3% and 25. 7% to the total torque transferred from the jet to the runner. Very few theoretical investigations on torque characterization have been reported. This compares well with some of the reported theoretical investigations and in contrast with others. Shepherd [24] that the first stage contributed 72% to the total torque generation while the remaining 28% was contributed by second stage. Balje [25] who found out that the first stage contributed 70% of the total torque and the second stage 30%. He assumed that the turbine takes half of the water through the runner and exhaust it through the other half. However, several flow profile investigations attest that flow stages are not equally partitioned as assumed by Balje.

Haimerl [26] found out that the first stage contributes 4.6 times the torque contributed in the first stage: thus 82% of the total torque is produced in the first stage and the remaining 18% contributed in the second stage. This is in contrast with theoretical results in this study. It should be pointed out that the differences in assumptions, runner size (radius ratio), and blade angle may contribute to having different theoretical results. The important observation is that the theoretical results show that the first stage contributes a bigger proportion of total torque compared to second stage.

The theoretical results further show that the relative toque transfer depends strongly on the geometry of the runner (square of the ratio of outside to inside diameters). This shows that as the inside runner diameter is made smaller, the contribution of the first stage is increasing more than the second stage. However, from optimization of the runner size, there is an optimum ratio of inside diameter to outside diameter to avoid back pressure and improve the performance of the turbine. Mockmore and Merryfield [4] calculated that this ratio should 0.66. Other documented experimental investigations such as those conducted by Varga [5], Horthersall [21] and Fiuzat & Akerkar [17] were conducted on turbines models having the radius ratio of 0.66 with satisfactory results. Others like those conducted by Johnson [16], Nakase [6] and Khosrowpanah [20] used radius ratio of 0.68 and maximum efficiency values were obtained. This study has used 0.69. Sonnek [27] concluded that the optimum radius ratio varies from 0.66 to 0.69. Therefore, it would mean that the practical values of radius ratio used are almost constant

and therefore alteration of the radius ratio to improve torque transfer in the second stage may not give maximum efficiency.

The results of torque transfer characterization as performed in this experiment using the strain gauge are shown in Table 7 and graphically in Figures 17 and 18.

It can be seen from Table 8 and the accompanying figures that at best efficiency point, (5m, 80% opening and 350 rpm – corresponding to 13.4 reduced speed), the first stage 57.2% of the total torque while the second stage contributes 42.8%. For both 350 rpm and 250 rpm speed, the first stage contributes relatively more to the total torque production than the second stage. However, it can be seen that as the amount of valve opening increases, the contribution of second stage increases, closer to being equal to the first stage contribution. At full valve opening, at 350 rpm, the second stage contributes more than the first while at 250 rpm the contribution of second stage is almost equal to that of first stage.

It can also be seen from the results that as the valve opening increases, the angle of runner utilization also increases. At best efficiency point (80% opening, 5m and 350 rpm), the angle of runner utilization is almost equal to 180 degrees, meaning half of the runner is used for torque generation. The torque contribution from second stage increases as the angle of runner utilization increases.

Table 7. Torque transfer characterization at 5m for speeds of 350 rpm and 250 rpm

Torque characterisation at 5m, 350rpm					Torque characterisation at 5m, 250rpm				
Valve opening (%)	Torque transfer First stage (%)	Torque transfer second stage (%)	Angle ψ (degrees)	Efficiency (%)	Valve opening (%)	Torque transfer First stage (%)	Torque transfer second stage (%)	Angle ψ (degrees)	Efficiency (%)
40	60.8	39.2	167	64	40%	63.6	36.4	185	62
60	57.7	42.3	176	73	60%	60.5	39.5	193	67
80	57.2	42.8	181	79	80%	58.2	41.8	201	69
100	46.3	53.7	241	76	100%	49.4	50.6	238	66.3
Average	55.5	44.5				57.9	42.1		

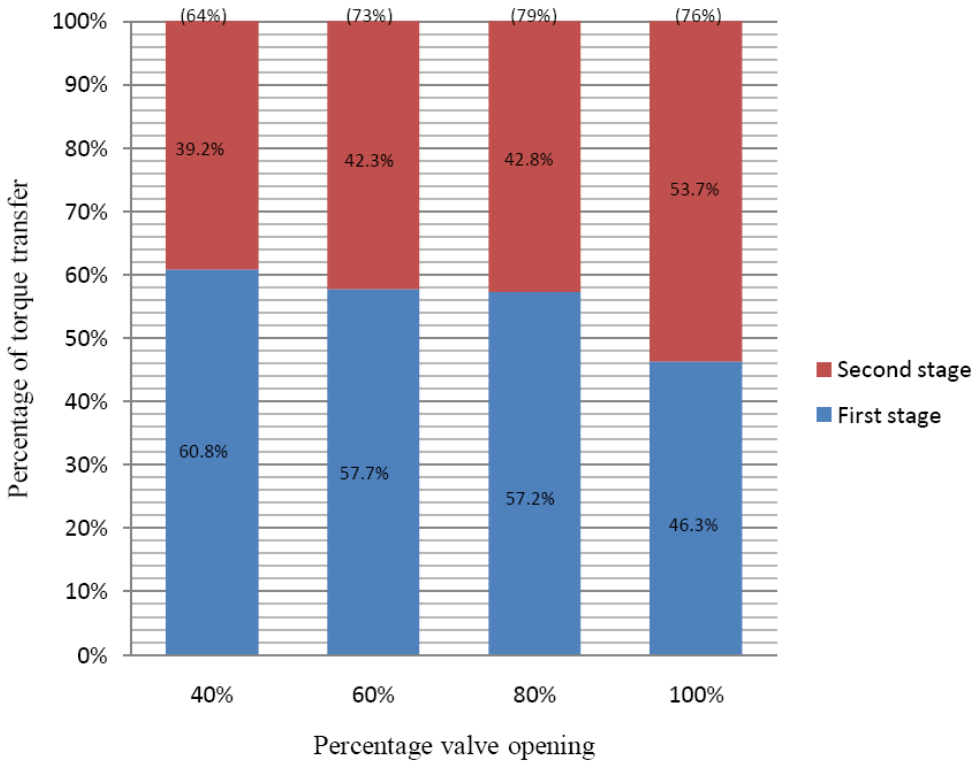

Figure 17. Torque transfer characterization at 5m head and 350 rpm rotational speed. The efficiency for the particular amount of valve opening are shown in brackets above the bar

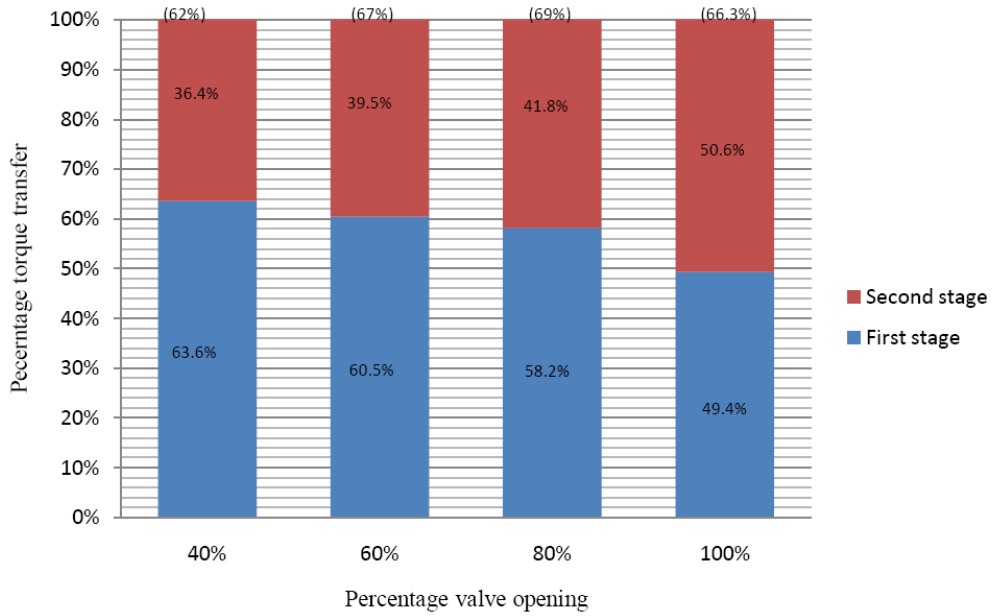

Figure 18. Torque transfer characterization at 5m head and 250 rpm rotational speed

The experimental results obtained in this experiment on relative torque production (57.2% first stage and 42.8% second) are in sharp contrast to the theoretically determined values (74.3% first stage and 25.7% second stage) of relative torque transfer at maximum efficiency. The discrepancy can be expected because the assumptions made during the theoretical analysis that there are no incidence losses and that the absolute velocity leaves the second stage of the runner without tangential component may not be practically true. Further, the theoretical was based on impulse principle of operation, but it has been shown that at best operation point the turbine had some degree of reaction. Therefore, the theoretical analysis might not have modeled the correct flow phenomenon in the actual turbine.

Not all of the flow from the nozzle crosses both stages (known as crossed-flow); some get entrained within the blades during the rotation of the runner. Since the entrained flow does not pass through the second stage, it does not contribute any torque in the second stage. This is another phenomenon that is not captured in the theoretical analysis, and may further explain the discrepancy between theoretical and experimental investigation on stage torque transfer characteristics.

The results of this experiment (at best efficiency conditions: speed 350, 5m, 80% valve opening) compare favorably with what Fiuzat and Akerkar got in 1991 [1] on Crossflow turbine model with a radius ratio of 0.68. Fiuzat and Akerkar experimented on two different configurations of the nozzle entry arcs: one with an admission angle of 90 degrees and the other with 120 degrees. For the 90 degree admission angle nozzle (like in this experiment), first stage contributed 53.8% of the total torque while the remaining 46.2% was contributed by the second stage: this experiment had 57.2% contribution from first stage and 42.8% from second stage. The Fiuzat and Akerkar [1] experiment was conducted with a maximum efficiency 78%.

The average torque transfer for all the valve openings in this experiment at 350 rpm is 55.5% for the first stage and 44.5% for the second stage. Fiuzat and Akerkar [1] found that the average contribution of first stage was 55% and for the second stage was 45% for the 90 degree admission angle nozzle.

It is also important to reiterate that in the current experiment, the simplified Crossflow model turbine nozzle admission angle is 90 degrees, the radius ratio is 0.69 and the maximum efficiency obtained was 79% at a reduced speed of 13.4. The experiment of Fiuzat and Akerkar [1], the maximum total efficiency (without flow extractor) was attained at a unit speed (defined as $\frac{ND}{\sqrt{H_e}}$) of 40 which if translated to reduced speed, as used in this experimental investigation, becomes 12.78. Therefore, it can be seen that the dynamic and physical parameters used in this experiment and that of Fiuzat and Akerkar [1] compare favorably.

However, the results of this experiment are in sharp contrast with what Durgin and Fay got in 1984 [8]. They found out that the first stage contributed 82% of the total torque; the remaining 18% was contributed by the second stage. The results are also in disagreement with what Andrade *et al*. [14]

obtained using numerical approach (computational fluid dynamics). They found out that the first stage contributes 68.5% of the total torque and the second stage 31.5% on a runner with a radius ratio of 0.68 and reduced speed of 12.7 (corresponding to a head of 35m, runner speed of 800rpm and outside diameter of 0.294m) with efficiency of 71%.

It is important for one to understand the methodologies that used to characterize torque transfer in other experimental investigations in order to the evaluate challenges and possible sources of disagreements in results. Durgin and Fay [8], Fiuzat and Akerkar [1] and possibly others used flow extraction methods to divert the crossed-flow out of the runner so that it does not strike the second stage. In this methodology, the first stage contribution to the total torque is obtained when the runner is being operated with the flow extractor. The difference in torque readings when the turbine operates without flow extractor and when it operates with flow extractor gives the second stage contribution to total torque transfer.

However, the flow extraction method is reported to have some drawbacks. The flow extractor can affect the performance of the runner by inducing back pressure [1]. This reduces the effective head on the nozzle and hence the power to be extracted from the jet. Further, the presence of the flow extractor can physically obstruct the rotation of the runner due to vibrations as the flow through the turbine increases. Durgin and Fay [8] were unable to perform the experiments at full load (corresponding to best efficiency) because of this problem: the results at full load were extrapolated from those at partial loads. This would partly explain why the Durgin and Fay [8] results are in sharp contrast with the Fiuzat and Akerkar [1] as well as the results from this experiment.

It is also important to state that the experiment of using the flow extractor does not measure torque directly but in terms of turbine efficiency. Therefore, it is important to make sure that the turbine is run at the same speed and head during both experiments (with flow extractor and without flow extractor) so that the ratio of efficiencies becomes the ratio of torques transferred in the runner at that operating condition. Further, the turbine efficiency involves mechanical power at the output shaft. The hydraulic efficiency which involves transfer torque from the jet to the blade is higher than the turbine efficiency because the hydraulic power extracted from the jet is always more than the shaftpower because of bearing losses. Since torque contribution from each stage is calculated from turbine efficiencies, then theoretically, there must be no bearing losses for the ratio of efficiencies to represent ratio of torques generated in the runner stages.

Therefore, it would seem that torque characterization using the strain gauge may give accurate results because it measures torque from first principles. It is to the knowledge of the authors that the methodology as used in this investigation of employing strain gauges to measure relative torque transfer using the impulse principle is first of its kind to be documented in scholarly articles on the Crossflow turbines. Fukutomi *et al*. [28] once employed use of strain gauges and slip rings on experimental investigation on the Crossflow turbine. However, it was for investigation of unsteady forces acting on the blades of the runner according to the momentum theory.

The interesting finding from torque characterization experiment is that the second stage is more significant in torque production than as theoretically predicted. Since the current design procedure is to optimize the flow angles at runner inlet (first stage) by controlling the valve (or guidevane), design efforts must be also directed towards improving the flow angles into the second stage. Incidence losses in the second stage (including those concerning jet colliding with the shaft) can be minimized by guiding the flow into the blades by inserting a flow guide inside of the runner. For best results, it would mean that the flow guider should be installed in the runner in the absence of the shaft that connects the two supporting discs. This would compromise the structural integrity of the runner; therefore studies such as those employing finite element analysis, need to be carried out to evaluate the effect of loading on the runner so as to obtain the correct runner size for structural integrity and hydraulic performance.

5.4 Characteristics of instantaneous torque generation in the runner

The plots of voltage signals generated from the strain gauge can be used to characterize the torque transfer further by looking at how the torque is generated in the blades with respect to time. It is a fact that torque can be generated when the jet impinges on the blades whether in form of splashes and the periodic nature of the voltage signal can give information about the quality of torque transfer in the stages.

By analyzing the plots in Figure 19, the following can be observed pertaining to torque transfer:

- The torque transfer is in a specific periodic pattern for a particular valve opening and runner speed. This implies that the instantaneous torque variation has an impact on structural strength of the blade (fatigue stress), vibrations on the shaft and quality of power production.
- With respect to the first stage, the peak (and area) for second stage relatively increases with valve opening for both runner speeds. This explains why the results that shows that the contribution of second stage increases with valve opening.
- The signal shows perturbations between the termination of second stage and initiation of the first stage. Theoretically, the runner spaces between the stages are not filled with water, this implies that the signal will be perfectly flat between stages. It can be seen that this is not the case generally, but the signal is characterized with perturbations. It can also be seen that these perturbations flatten out with runner speed of 250rpm as compared with the speed of 350 rpm at all valve openings. It can also be seen that for runner speed of 350 rpm, at 80% opening, the perturbations show a degree of flattening out. The source of these perturbations can be due to the water splashing which may hit either side of the blade as it rotates to reach the start position of the first stage. The splash may come from the jet hitting the shaft. It can also be argued that the crossed flow (inter-stage flow) come out from the first stage blades with different directions of the absolute velocities and they tend to collide inside of the runner, creating splashes.
- For the first stage at 100% valve opening for both speeds, it can be seen that the signal in the first stage has clearly identified perturbations. These perturbations may not be associated with water splashes but possibly with wrong relative velocity flow angle with respect to the design blade angle of 30^0. At 100% valve opening, the first stage inlet covers a relatively large area of the runner periphery. The flow, due to the interaction with the nozzle entry arc, may not approach the first stage with a homogenous angle of attack that is equal to the design value 16^0. This situation makes the jet hit the blades with wrong relative velocity flow angle causing flow separation which induces wakes. Wakes, which are exacerbated if the runner is operated outside the best efficiency point, reduce torque production. The description of wakes on production of perturbations in the flow angles was also stated by Andrade *et al*. [14].
- At 40% valve opening for 350rpm speed, the second stage is not clearly demarcated. This implies that the turbine effectively operates as a one stage turbine and the jet exchanges momentum (generates torque) only for a small duration of time. This is typical for pure impulse turbine like Pelton Wheel. This validates the observation from performance tests that at smaller valve openings, the Crossflow turbine operates as a pure impulse turbine.

6. Conclusions and recommendations

The key conclusions and recommendations on this experimental study can be stated as follows:

- A simple flap controlled with a screw as a valve can replace a traditional guide-vane in a Crossflow turbine technology without affecting its performance. The maximum measured efficiency of 79% compares favorably with reported performance levels of small scale Crossflow turbines. This finding can help to reduce the unit cost of Crossflow turbine.
- The simplified Crossflow operates optimally with a varied flow from the best efficiency point.
- Though designed as an impulse turbine, simplified Crossflow turbine under study performs well with a degree of reaction at larger valve openings. The experiments have also validated the reported observations that a modified Crossflow turbine where part of the nozzle wall follows the runner housing closely has some degree of reaction.
- The experiment has demonstrated use of strain gauge in an experiment to characterize torque in the two stages of the runner. This is addition to knowledge because, from the knowledge of the authors, previous investigators employed flow extraction techniques to determine the relative torque transferred in the stages. Flow extraction techniques have a disadvantage of flow extractor interfering with the rotation of the runner.
- Experimental results on torque characterization are in contrast with the theoretically obtained values. This calls for the modification of the theory. Further, experimental results show that the second stage is also significant in torque production. While the flow angles are controlled at the entrance of the first stage by the valve and nozzle wall, they are not at the entrance to the second stage. Is therefore recommended to put a structure inside of the runner to control jet entry into the second stage. This may require removal of the shaft that connects the two discs where the blades are attached. Studies

are recommended to determine the structural strength of the runner blade assembly in the absence of the shaft connecting the two discs.

- Further analysis on the strain gauge signals reveals instantaneous characteristics of toque generation. Clear demarcated stages can identified from the plots as well as the trends in torque generation at a particular valve opening and speed: therefore they give some information the nature of flow in the turbine runner. There is need for numerical analysis on the flow pattern inside the turbine so as to complement the findings from this experiment.

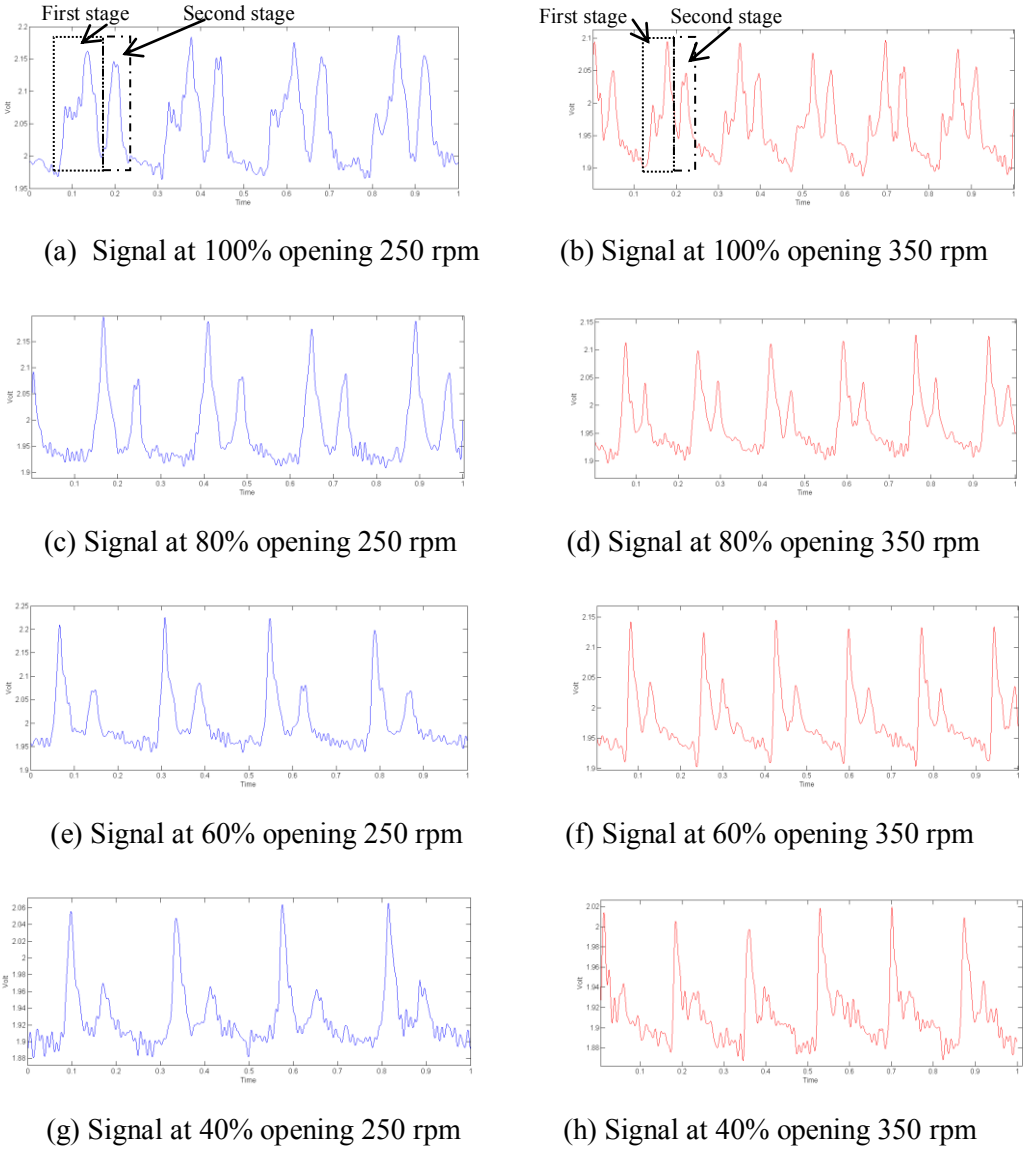

(a) Signal at 100% opening 250 rpm (b) Signal at 100% opening 350 rpm

(c) Signal at 80% opening 250 rpm (d) Signal at 80% opening 350 rpm

(e) Signal at 60% opening 250 rpm (f) Signal at 60% opening 350 rpm

(g) Signal at 40% opening 250 rpm (h) Signal at 40% opening 350 rpm

Figure 19. Trends in filtered voltage signal for various valve openings at 5m for 250 rpm and 350 rpm runner speeds

Acknowledgement

The authors appreciate the support from NORAD under the Energy and Petroleum (EnPe) Program for funding this research at Waterpower Laboratory, Department of Energy and Process Engineering, Norwegian University and Technology.

References

[1] Fiuzat A., Akerkar B. Power output of two stage of Crossflow turbine. Journal of energy engineering, 1991, vol 117, no. 2, pp: 57-70, American Society of Civil Engineers (ASCE).

[2] Cobb B., Sharp K. Impulse (Turgo and Pelton) turbine performance characteristics and their impact on pico-hydro installations. Journal of Renewable Energy, 2013, volume 50, pp: 959-964.
[3] Anagnostopoulos J., Papantonis D. Flow modeling and runner design optimization in Turgo water turbines. International Journal of Engineering and Applied Sciences, 2008, volume 4, Issue 3, pp: 136 -141.
[4] Mockmore C., Merryfield F. The Banki water-turbine. Engineering Bulletin Series Number 25, Oregon State University, Corvallis, United States of America, 1949.
[5] Varga J. Tests with the Banki water turbine. Journal of the Hungarian Academy of Sciences, 1959, vol. pp: 779-102.
[6] Nakase Y., Fukutomi J., Watanabe T., Suetsugu T., Kubota T., Kushimoto S. A study of the cross-flow turbine, effects of nozzle shape on its performance. Journal of Small hydro-power fluid machinery, American Society of Mechanical Engineers (ASME), 1982, pp: 29-133.
[7] Meier U., 1982. Design of Crossflow Turbine BYS/T1: (Working Drawings). Document available from Swiss Center for Appropriate Technology, Varnbuelstrasse 14, CH-9000 St. Gallen, Switzerland. Also available online at http://www.cd3wd.com/cd3wd_40/JF/430/22-502.pdf . Accessed on 2nd February, 2013.
[8] Durgin W., Fay W. Some Fluid Flow Characteristics of a Crossflow Type Hydraulic Turbine. In proceedings of American Society of Mechanical Engineers (ASME) Winter Annual Meeting on small hydropower fluid machinery, New Orleans, USA, 1984.
[9] Khosrowpanah S., Fiuzat A., Albertson M. Experimental study of the Crossflow turbine. Journal of Hydraulic Engineering, 1988, vol. 114, no. 3, pp: 299-314, American Society of Civil Engineers (ASCE).
[10] Desai V., Aziz N. Parametric evaluation of Crossflow turbine performance. Journal of energy engineering, 1994, vol 120, issue no. 1, pp: 17-34, American Society of Civil Engineers (ASCE).
[11] Totapally H., Aziz M. Refinement of Crossflow turbine design parameters. Journal of Energy Engineering, 1994, vol.120, issue no. 3, pp: 133-147, American Society of Civil Engineers (ASCE).
[12] Barglazan M. About design optimization of Crossflow hydraulic turbine. Scientific bulletin of the Polytechnic University of Timisoara, Transaction on Mechanics, 2005, vol 50, issue 64, pp: 24-28.
[13] Choi Y., Lim J., Kim Y., Lee Y. Performance and internal flow characteristics of a Crossflow hydro turbine by the shapes of the nozzle and runner blade. Journal of Fluid Science and Technology, 2008, vol.3, No. 3, The Japan Society of Mechanical Engineers (JSME).
[14] Andrade J., Curiel C., Kenyery F., Aguillon O., Vasquez A., Asuaje M. Numerical Investigation of the Internal Flow in a Banki Turbine. International Journal of Rotating Machinery, 2011, vol. 2011, article ID 841214, 12 pages.
[15] Sammartano V., Arico C., Carravetta A., Fecarotta O., Tucciarelli T. Bank-Michell optimal design by computational fluid dynamic testing and hydynamic analysis. Energies, 2013, vol. 6, pp: 2362-2385; doi:10.3390/en6052363, MDPI - Open Access Publishing.
[16] Johnson W., Ely R., White F. Design and testing of an inexpensive cross-flow turbine. In Proceedings of American Society of Mechanical Engineers (ASME) annual symposium on small hydropower fluid machinery, New York, USA, 1982.
[17] Fiuzat A., Akerkar B. The use of interior guide tube in crossflow turbines. In Proceedings of the American Society Civil Engineers (ASCE) meeting on Waterpower, ASCE, New York, United States of America, 1989, pp 1111-1119.
[18] International Electrotechnical Commission (IEC). Hydraulic turbine, storage pumps and pump-turbine model acceptance tests. Published by IEC 1999, Geneva, Switzerland.
[19] Ossberger GmbH + Co. Ossberger Turbine. Available from company website: http://www.ossberger.de/cms/pt/hydro/ossberger-turbine/. Accessed on 16 October, 2013.
[20] Khosrowpanah S. Experimental study of the Crossflow turbine. PhD dissertation, Colorado State University, Colorado, United States of America, 1984.
[21] Hothersall R. A review of the cross-flow turbine. In Proceedings of American Society of Civil Engineers (ASCE) on Waterpower, New York, N.Y., 1985, vol. 2, page 914.
[22] Ott R., Chappel J. Design and efficiency testing of a cross-flow turbine. In Proceedings of American Society of Civil Engineers (ASCE) on Waterpower, New York, N.Y., 1989, 1534-1539.
[23] Olgun H. Investigation of the performance of the Crossflow Turbine. International Journal of Energy Research, 1998, issue 22, pp 953 – 964.

[24] Shepherd D. Principles of Turbomachinery. Prentice Hall PTR, New Jersey United States of America, ISBN-10: 0024096601, 1956.
[25] Balje O. Turbomachines: A Guide to design, selection and theory. Published by John Wiley and Sons, New York, United States of America, ISBN 10: 0471060364, 1981.
[26] Haimerl L. The Crossflow turbine. Water power, 1960, volume 22, issue number 1, pp 5-13.
[27] Sonnek E. The theory of the Crossflow turbine. Berlin Verlag von Julius Springer, 1923.
[28] Fukutomi J., Nakase Y., Ichimiya M., Ebisu H. Unsteady Forces on a blade in a Crossflow turbine. Japanese Society of Mechanical Engineers (JSME) International Journal, 1995, volume 38, no. 3, series B, pp: 404-410.

Chiyembekezo S. Kaunda is an energy lecturer and an energy consultant. He is an academic member of staff at the University of Malawi but currently pursuing a sandwiched Ph.D in microhydro systems at University of Dar es Salaam and Norway University of Science and Technology. He has an MSc in Thermofluids and Energy Systems obtained from Kwame Nkrumah University of Science and Technology, Kumasi, Ghana in 2006. Has five publications in the area of small-scale hydropower systems. He has reviewed several Government of Malawi documents on energy and environment as well as UNIDO World Small Hydropower Development Report (2013). Has conducted consultancies in energy project evaluation and climate change mitigation in Malawi. He has attended training workshops in hydropower and environment, energy and development, rural electrification and climate change. Mr. Kaunda's main research interests are in renewable energy, environment and climate change.
E-mail address: kaundas@gmail.com or skaunda@poly.ac.mw

Cuthbert Z. Kimambo is an Associate Professor of renewable energy at University of Dar es Salaam, Tanzania. He has an MSc and Ph.D in Mechanical Engineering from Reading University and London City University, United Kingdom, respectively. He lectures renewable energy and supervises many MSc and Ph.D students in energy engineering. Prof. Kimambo's main research interests are in renewable energy especially solar, hydro and wind. He has several publications in renewable energy. He is an outgoing Chairperson for the Tanzanian Renewable Energy Agency.
E-mail address: kimambo@udsm.ac.tz

Torbjorn K. Nielsen a full Professor of hydropower at Norwegian University of Science and Technology (NTNU) and is in charge of the Waterpower Laboratory. He is an expert in hydropower turbine design and transient analysis. Has conducted several consultancies in these areas. He lectures and supervises several MSc and PhD students. Prof. Nielsen's main research interests include design of turbomachinery and their verification using numerical methods as well pressure transient analysis in hydropower systems.
E-mail address: torbjorn.nielsen@ntnu.no

